Enhanced electron mobility in epitaxial (Ba,La)SnO_3 films on $BaSnO_3$(001) substrates

Woong-Jhae Lee,[1,a)] Hyung Joon Kim,[1,a)] Egon Sohn,[1] Tai Hoon Kim,[1] Ju-Young Park,[1] Woanseo Park,[2] Hyunhak Jeong,[2] Takhee Lee,[2] Jin Hyeok Kim,[3] Ki-Young Choi,[1] and Kee Hoon Kim[1,2,b)]

[1]*Center for Novel States of Complex Materials Research, Department of Physics and Astronomy, Seoul National University, Seoul 151-747, South Korea*
[2]*Institute of Applied Physics, Department of Physics and Astronomy, Seoul National University, Seoul 151-747, South Korea*
[3]*Department of Materials Science and Engineering, Chonnam National University, Gwangju 500-757, South Korea*

(Received 28 November 2015; accepted 10 February 2016; published online 23 February 2016)

We report the growth of $Ba_{1-x}La_xSnO_3$ ($x = 0.00$, 0.005, 0.01, 0.02, and 0.04) thin films on the insulating $BaSnO_3$(001) substrate by pulsed laser deposition. The insulating $BaSnO_3$ substrates were grown by the Cu_2O-CuO flux, in which the molar fraction of $KClO_4$ was systematically increased to reduce electron carriers and thus induce a doping induced metal-insulator transition, exhibiting a resistivity increase from $\sim 10^{-3}$ to $\sim 10^{12}\,\Omega$ cm at room temperature. We find that all the $Ba_{1-x}La_xSnO_3$ films are epitaxial, showing good in-plane lattice matching with the substrate as confirmed by X-ray reciprocal space mappings and transmission electron microscopy studies. The $Ba_{1-x}La_xSnO_3$ ($x = 0.005$–0.04) films showed degenerate semiconducting behavior, and the electron mobility at room temperature reached 100 and 85 $cm^2\,V^{-1}\,s^{-1}$ at doping levels 1.3×10^{20} and $6.8 \times 10^{19}\,cm^{-3}$, respectively. This work demonstrates that thin perovskite stannate films of high quality can be grown on the $BaSnO_3$(001) substrates for potential applications in transparent electronic devices. © *2016 AIP Publishing LLC*. [http://dx.doi.org/10.1063/1.4942509]

For more than several decades, transparent conducting oxides (TCOs) and transparent oxide semiconductors (TOSs) have been used in applications such as solar cells, flat panel displays, light emitting diodes, and transparent electronic devices. Some of binary oxide systems based on ZnO, In_2O_3, and SnO_2 have been mostly used for demonstrating key performance for device applications: p-n junctions, field-effect transistors, and UV lasers.[1–12] On the other hand, there is growing interest toward new TOSs with the perovskite structure, in which carrier doping and structural modification can be more flexible than those conventional TOSs made of binary oxides. Perovskite TOSs can also provide an opportunity to realize versatile functionality, e.g., ferroelectricity and two-dimensional electron gas.[13,14] Titanium-based perovskites, such as doped-$SrTiO_3$ (STO) and $CaTiO_3$,[15,16] have been investigated toward this direction. However, those perovskite titanates generally showed much lower electron mobility (μ) than doped binary oxides at room temperature.

It was recently found that donor-doped $BaSnO_3$ (BSO) with the cubic perovskite structure, e.g., $Ba_{1-x}La_xSnO_3$ (BLSO) single crystals, becomes n-type TOSs and TCOs with high μ ($\sim 300\,cm^2\,V^{-1}\,s^{-1}$),[17,18] wide band gap (>3.1 eV),[18,19] and excellent thermal stability.[17,20] The value of $\mu = \sim 300\,cm^2\,V^{-1}\,s^{-1}$ at room temperature is the highest among other TCOs in a degenerate semiconductor regime. One of next necessary steps for applications is to grow high-quality thin films that exhibit high μ as in the single crystals even in a low doping regime. Until recently, most of reported BLSO films were grown on STO(001) substrates (BLSO/STO), of which lattice constant (~3.905 Å) has a large mismatch of +5.40% with that of BSO(001) (~4.116 Å). As a result, lots of grain boundaries and threading dislocations were found to exist in BLSO/STO.[17,18,21] Naturally, the best μ value was still limited to ~ 40–$60\,cm^2\,V^{-1}\,s^{-1}$ at high carrier concentrations (n) ($>2 \times 10^{20}\,cm^{-3}$) and was smaller than $30\,cm^2\,V^{-1}\,s^{-1}$ in a low n regime ($<7 \times 10^{19}\,cm^{-3}$). This is in sharp contrast with the behavior of single crystals exhibiting a nearly carrier-independent μ of ~ 200–$300\,cm^2\,V^{-1}\,s^{-1}$.[18] More recently, BLSO/STO with $\mu = \sim 60$–$80\,cm^2\,V^{-1}\,s^{-1}$ was reported in relatively thick films (300 nm) and in films with a BSO buffer layer.[22] However, there still exist lots of rooms for improving μ of thin stannates films in broad doping regimes, particularly at the low dopant regime.

Finding a suitable substrate to grow BLSO thin films remains as one of major challenges. An ideal substrate would be the insulating BSO single crystal itself, as its lattice constant matches well with those of BLSO within 0.08%.[19,23] However, it was recently found that BSO single crystals grown by the Cu_2O flux usually became oxygen deficient to produce n-type carriers of $\sim 10^{19}\,cm^{-3}$.[23] Moreover, the crystals grown by the PbO-based flux contained considerable amount of Pb impurities to reduce intrinsic mobility.[19] Alternative efforts to grow BSO single crystals with an optical mirror furnace have so far failed due to high evaporation and decomposition of constituent elements.

In this letter, we report the growth of highly insulating BSO single crystals with lateral areas close to $\sim 2 \times 2\,mm^2$. Using the grown single crystals as a substrate in combination with fine polishing, we could grow epitaxial BLSO films on

a)W.-J. Lee and H. J. Kim contributed equally to this work.
b)Electronic mail: khkim@phya.snu.ac.kr

BSO(001) substrates (BLSO/BSO) to find enhanced μ in a broad doping range ($6.8 \times 10^{19} \leq n \leq 5.3 \times 10^{20}\,\mathrm{cm}^{-3}$) at room temperature as compared with those grown on STO(001) substrates.

For the growth of single crystals, polycrystalline BSO powders and a mixture of CuO and Cu_2O flux with an additional compound $KClO_4$ were put into a Pt crucible with a molar ratio of $BaSnO_3$:CuO:Cu_2O:$KClO_4$ = 1:22.4:27.6:y ($0.0 \leq y \leq 3.0$). It was fired in air up to 1230 °C and then slowly cooled to 1070 °C. We polished BSO(001) crystals to have a flat surface along the c-plane using a polishing machine (Allied High Tech Products, Inc.), polishing cloths, and colloidal silica suspensions. BLSO thin films (90 nm) were deposited by pulsed laser deposition with a KrF excimer laser ($\lambda = 248$ nm) with a laser fluence of $\sim 1.0\,\mathrm{J/cm}^{-2}$, using BLSO ($x = 0.00$, 0.005, 0.01, 0.02, and 0.04) targets. Insulating BSO(001) substrates grown with $KClO_4$ ($y = 2.0$) were used and the deposition was made in an O_2 pressure of 100 mTorr at 790 °C. To measure Hall effect of BLSO/BSO(001) at room temperature, we employed the Van der Pauw method. We investigated structural properties of BSO crystals and BLSO/BSO using high-power X-ray diffractometers (Empyrean, PANalytical and AXS D8, Bruker). The former was used for θ–2θ scans and rocking curves (ω-scans), while the latter was used for rocking curves and reciprocal space mapping (RSM). We confirmed that the rocking curves obtained from the Empyrean in a channel-reducing mode provide the same results from the AXS D8 in an open detector mode. To estimate actual La-doping levels in the grown film, we performed electron-probe microanalysis (EPMA) with spatial resolution of several micrometers. Surface morphology was studied by atomic force microscopy (AFM) (NX10, Park Systems). Transmission electron microscopy (TEM) (JEM-3000F, JEOL) experiment was performed for investigation of local structural properties of BLSO/BSO(001).

We could grow highly insulating BSO single crystals by using mixed CuO and Cu_2O powders as a main flux with a molar ratio of CuO:Cu_2O = 39:61. In the given molar ratio, the CuO + Cu_2O flux forms an eutectic melting point at 1090 °C,[24] which is lower than the melting temperature of Cu_2O flux only (1230 °C) by 140 °C.[17,18,24] Hence, the temperature window of the crystal growth has been widened, possibly explaining why crystal sizes have increased overall ($\sim 2 \times 2\,\mathrm{mm}^2$). We also found that the best molar ratio of (CuO + Cu_2O):$BaSnO_3$ for growing single crystals is ~50:1. $KClO_4$ has been used before as an oxidizer during the solid state synthesis under high pressure.[25,26] It was thus expected that $KClO_4$ could either provide additional oxygen to reduce oxygen deficiency (V_O) or potassium ions (K^+) as acceptors to compensate the n-type carriers by V_O in the BSO crystals. Based on this motivation, the molar ratio of $KClO_4$ was systematically varied to determine the optimal condition for obtaining the most insulating transport properties; the best molar ratio of $BaSnO_3$:CuO + Cu_2O:$KClO_4$ turned out to be 1:50:2. The EPMA study on BSO crystals revealed that they contained detectable amount of K impurities ($\sim 1.4 \times 10^{19}\,\mathrm{cm}^{-3}$),[27] indicating that electron carriers were partially reduced by compensation of hole carriers from K.

Figure 1(a) displays the X-ray θ–2θ scan of ground BSO single crystals grown with $KClO_4$ ($y = 2.0$) (BSO($y = 2.0$)),

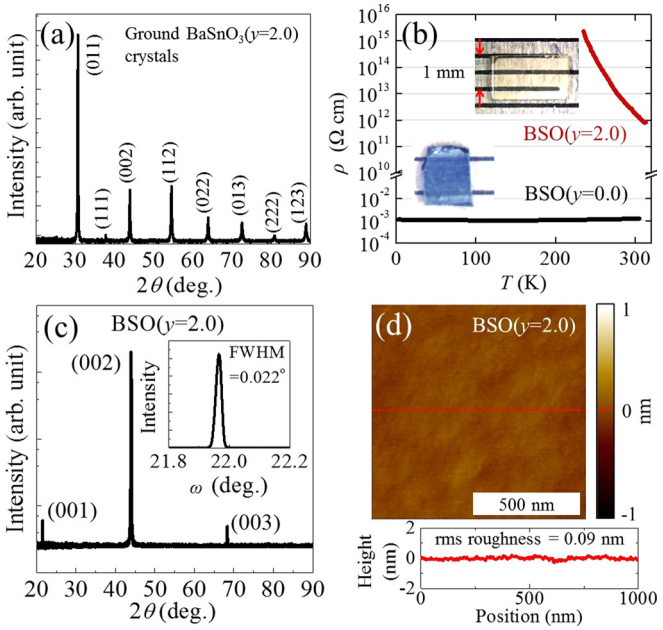

FIG. 1. (a) X-ray θ-2θ scan results of ground powders of $BaSnO_3$($y = 2.0$) single crystals (BSO($y = 2.0$)) grown by the flux method, which uses a mixture of cupric oxides and $KClO_4$ as a flux with a molar ratio of $BaSnO_3$:CuO:Cu_2O:$KClO_4$ is 1:22.4:27.6:y ($0.0 \leq y \leq 3.0$). (b) Electrical resistivity of BSO($y = 0.0$) and BSO($y = 2.0$). (c) The X-ray θ-2θ profile of the BSO($y = 2.0$). The inset shows the rocking curve of the (002) peak. (d) Surface morphology and height of the annealed BSO($y = 2.0$) substrate after polishing. Bottom panel shows the height profile along the dotted solid line.

exhibiting the peaks expected in the cubic perovskite structure only. BSO($y = 2.0$) showed a high electrical resistivity (ρ) of $\sim 1 \times 10^{12}\,\Omega\,\mathrm{cm}$ at room temperature, while BSO crystals without $KClO_4$ ($y = 0.0$) (BSO($y = 0.0$)) showed a low ρ of $\sim 1\,\mathrm{m}\Omega\,\mathrm{cm}$ and metallic behavior (Fig. 1(b)). Consistent with this, BSO($y = 2.0$) became more transparent than BSO($y = 0.0$) (inset of Fig. 1(b)). The X-ray θ–2θ scan on the flat surface of the grown BSO($y = 2.0$) exhibited only (00l) peaks with the out-of-plane lattice constant (c) of ~4.116 Å, confirming good alignment of the {001} plane (Fig. 1(c)). The inset of Fig. 1(c) shows the rocking curve measured at the 2θ angle of (002) Bragg peak of BSO($y = 2.0$). Upon fitting with the pseudo-Voigt function, quite a small, full-width-at-half-maximum (FWHM) of 0.022° was obtained, proving high degree of crystallinity. The AFM study of as-polished BSO($y = 2.0$) resulted in a maximum height difference of ~0.9 nm and root-mean-square (rms) roughness of ~0.3 nm. Moreover, after annealing at 1000 °C under air for 1 h, the rms roughness was reduced to become as low as 0.09 nm (Fig. 1(d)). Given that the rms roughness of commercial STO substrates is typically around 0.1 nm, the polishing and thermal annealing seems to be an effective method to obtain smooth surface in the BSO substrate.

Figures 2(a) and 2(b) show AFM images of BLSO/BSO ($x = 0.01$ and 0.04) thin films. Their maximum height difference and rms roughness were found to be about ~0.8 nm and ~0.24–0.27 nm, respectively, demonstrating that smooth films could be grown on BSO substrates. The θ–2θ scans of BLSO/BSO ($x = 0.00$, 0.01 and 0.04) (Fig. 2(c)) showed that they were grown along (00l) directions without undesired phases. The inset shows expanded 2θ profiles around (002) Bragg reflection of the films, showing systematic shifts toward lower angles as x is increased. This observation implies

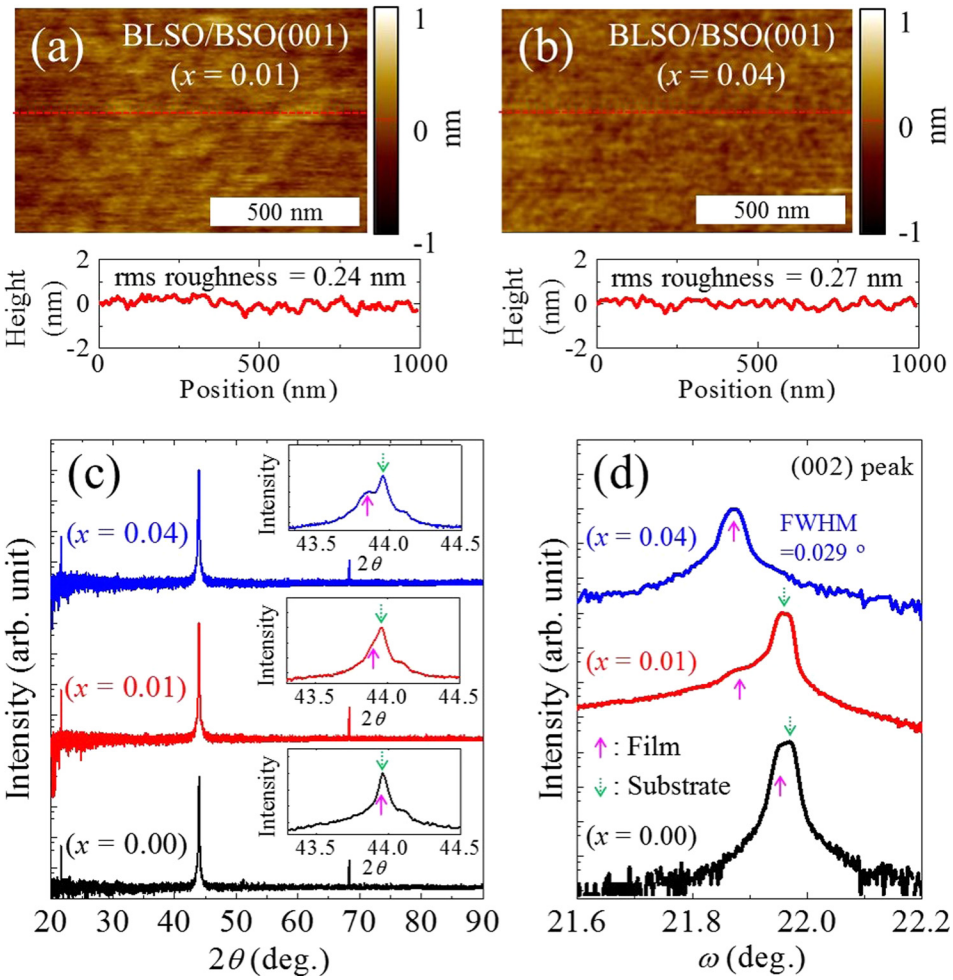

FIG. 2. (a) and (b) show the surface morphology and heights of the $Ba_{1-x}La_xSnO_3$ ($x = 0.01$ and 0.04) films, respectively. Bottom panels show the height profiles along the dotted solid lines. (c) The θ-2θ scan results of the $Ba_{1-x}La_xSnO_3$ films. The inset shows the θ-2θ scan near (002) peaks. Film peaks are indicated with the solid arrows, while the peaks related with the BSO substrate are shown as dotted arrows. (d) The rocking curves measured at the (002) peaks of the films.

that the out-of-plane lattice constant in $x = 0.00$ and 0.01 films, which is close to that of BSO substrates, is expanded as x is increased from 0.00 and 0.01 to 0.04. Figure 2(d) shows rocking curves measured at the center of (002) Bragg peaks of three films ($x = 0.00$, 0.01, and 0.04). We find that the rocking curves of BSO/BSO and BLSO/BSO ($x = 0.01$) films are screened by the contribution of substrates or exhibit only a shoulder-like feature, respectively, making it difficult to obtain FWHM of those films. However, the rocking curve of the BLSO ($x = 0.04$) film is well separated from that of substrates so that FWHM could be obtained to be as small as 0.029°, confirming the good crystallinity. In comparison, we recall in previous reports that FWHMs in the ω-scans of BLSO films grown on STO or MgO were 0.09°–1.0°.[18,28,29] Those results clearly indicate that thin BLSO films grown on the BSO substrate have better crystallinity than those grown on STO or MgO.

To better understand structural evolutions with La doping, we investigated X-ray RSM. Figure 3(a) displays (103) reflection of the BSO substrate, forming only one spot in the (Q_x, Q_z) plane. Calculations of in-plane lattice constant (a) and c from the spot position resulted in a nearly same value of 4.116 Å, being consistent with the cubic symmetry of BSO substrates. Figure 3(b) shows RSM of the BLSO/BSO ($x = 0.04$), revealing that the Q_x of the film spot is nearly same as that of the BSO substrate, while the Q_z of the film spot is clearly smaller than that of the BSO substrate. From this, it is concluded that the BLSO ($x = 0.04$) film has $a = \sim 4.116$ Å, almost same as the substrate, while $c = 4.126$ Å of the film is increased by +0.24% as compared with that of the substrate. This implies that the in-plane of the BLSO ($x = 0.04$) film is subject to compressive strain to have the same a value with the substrate, while its c-axis is expanded than that of the substrate to meet the Poisson relation. Note that the BLSO ($x = 0.03$ and 0.04) polycrystals are known to have generally larger lattice constants (4.1175–4.1181 Å) than that of undoped one (4.1151–4.1160 Å), according to the literatures.[18,19,30] On the other hand, nearly one spot could be identified in the RSM of the BLSO ($x = 0.01$) film (Fig. 3(c)), implying that films with low $x \leq 0.01$ have almost same lattice constants with BSO substrates along both in-plane and out-of-plane directions. The present RSM results thus indicate that BLSO films grown on the BSO substrate may have increasing compressive strain as the La doping level is increased. This can be understood because bulk BLSO shows the progressive increase of pseudo-cubic lattice constants with La doping as electron carriers fill up antibonding states of Sn 5s character.[18]

To investigate local structural properties more directly, we performed the TEM study. Figures 3(d) and 3(e) show cross-sectional TEM images of the BLSO/BSO ($x = 0.005$). We could not find any dislocations or grain boundaries in a bright field image covering a wide area of film cross-section over $\sim 100 \times 500\,nm^2$ (Fig. 3(d)). The high-resolution image near the interface also demonstrates that the lattice periodicity of the BLSO film almost perfectly matches that of the BSO substrate; fifteen layers of (101) planes in the BSO substrate

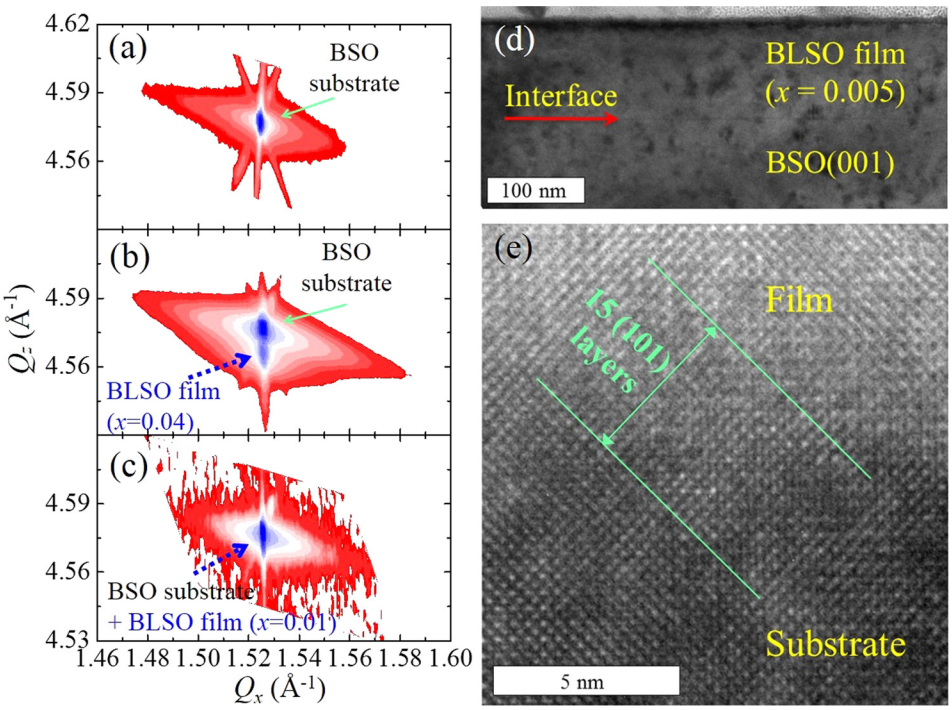

FIG. 3. Reciprocal space maps of the (103) reflection for the (a) $BaSnO_3$(001) substrate, (b) $Ba_{0.96}La_{0.04}SnO_3$/$BaSnO_3$(001), and (c) $Ba_{0.99}La_{0.01}SnO_3$/$BaSnO_3$(001). (d) and (e) show low- and high-magnification cross-sectional TEM images at the film-substrate interface of $Ba_{0.995}La_{0.005}SnO_3$/$BaSnO_3$(001), respectively.

have the same distance in the BLSO film (Fig. 3(e)). With such a good lattice match, we could not distinguish well even the interface between the substrate and the film, supporting that the high quality epitaxial BLSO films are realized on the BSO(001) substrate.

Figures 4(a) and 4(b) summarize ρ and μ as a function of n at room temperature in BLSO/BSO and reported BLSO/STO.[18] Red, blue, orange, and magenta circles represent data points from BLSO/BSO grown by sintered $Ba_{1-x}La_xSnO_3$ targets with $x = 0.005$, 0.01, 0.02, and 0.04, respectively. Although there exist scatterings in data points among films, the measured n (ρ) values of BLSO/BSO are systematically increased (decreased) in proportional to the La-doping level in targets. Moreover, they are close to carrier numbers expected from those targets. An EPMA study on one of BLSO/BSO ($x = 0.005$) also showed that La dopants had small variation over the 10 different spots measured and the averaged value was $x = 0.0061 \pm 0.0011$, being close to the nominal doping level of the target. Figure 4(b) shows that the measured μ of BLSO/BSO is $\sim 75\,cm^2\,V^{-1}\,s^{-1}$ at a high n regime ($\sim 5.0 \times 10^{20}\,cm^{-3}$) and $\sim 80-100\,cm^2\,V^{-1}\,s^{-1}$ in a low n regime ($\leq 1.0 \times 10^{20}\,cm^{-3}$). The slightly increasing trend of μ with decrease of n is somewhat similar to the behavior observed in BLSO single crystals, in which ionic scattering due to La^{3+} ions became dominant scattering sources.[17,23] In contrast, BLSO/STO showed clear μ decrease with the decrease of n due to strong carrier scatterings at grain boundaries and dislocations.[17,18,21] Our observation implies that the μ of BLSO thin films on BSO(001) substrates is not dominated by scatterings from dislocations/grain boundaries. Therefore, the enhanced μ values and the nearly n-independent behavior of μ should represent merits of epitaxial BLSO films on BSO substrates with much reduced structural defects without threading dislocations/grain boundaries.

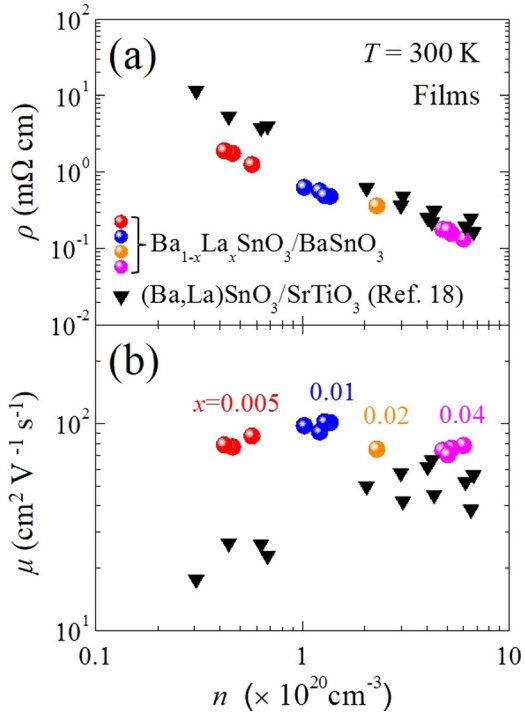

FIG. 4. (a) Electrical resistivity (ρ) and (b) electron mobility (μ) *vs.* carrier density (n) plots for $Ba_{1-x}La_xSnO_3/BaSnO_3$(001) films (circles). ρ and μ *vs.* n of $Ba_{1-x}La_xSnO_3/SrTiO_3$(001) films (triangles) are from Ref. 18. Reproduced with permission from Kim *et al.*, Phys. Rev. B, **86**, 165205 (2012). Copyright 2012 American Physical Society.

It should be noted that μ values in BLSO/BSO correspond to the largest one among perovskite TCO films at room temperature. Furthermore, those μ values are comparable to or even larger than those of other familiar TOS films at a similar n regime.[31–33] Yet, they are still three times smaller than the best-known values in BLSO single crystals.[18] This means that the BLSO/BSO thin films have extra-scattering sources as compared with the single crystals. Inferred from the extensive research outcome for growing

high quality $SrTiO_3$ thin films,[34–36] we expect that one plausible reason for having extra scattering in the film could be point defects, coming from cation vacancies or cation site mixing. Therefore, it is worthwhile to investigate systematically the effect of point defects on the μ behavior of BLSO thin films in future studies.

In summary, we have reported the growth of highly insulating BSO single crystals based on the flux method employing cupric oxides and $KClO_4$ as flux materials. Using grown BSO(001) single crystals as a substrate, we have grown epitaxial $Ba_{1-x}La_xSnO_3$/BSO(001) ($0.005 \leq x \leq 0.04$) films. The resultant μ at room temperature reached as high as $\sim 100\,cm^2\,V^{-1}\,s^{-1}$, and showed slightly increasing behavior with the decrease of n, qualitatively similar to the single crystal behavior. Our results point to an unprecedented opportunity for growing high-quality BSO and BLSO films on BSO(001) substrates. This possibility, along with the superior thermal stability of BLSO materials,[17] suggests that BLSO films might be useful for transparent electronic devices operating under high-power and high-temperature conditions.

This work was financially supported by the National Creative Research Initiative (2010-0018300) and the Korea-Taiwan Cooperation Program (0409-20150111) through the NRF of Korea funded by the Ministry of Education, Science and Technology. T.L. acknowledges the financial support of the National Creative Research Laboratory Program (Grant No. 2012026372), funded by the Korean Ministry of Science, ICT & Future Planning. RSM study has been performed using a high-power X-ray diffractometer (AXS D8, Bruker) at IBS Center for Correlated Electron Systems, Seoul National University.

[1]D. S. Ginley and C. Bright, MRS Bull. **25**, 15 (2000).
[2]A. J. Freeman, K. R. Poeppelmeier, T. O. Mason, R. P. H. Chang, and T. J. Marks, MRS Bull. **25**, 45 (2000).
[3]T. Minami, MRS Bull. **25**, 38 (2000).
[4]H. Hosono, Thin Solid Films **515**, 6000 (2007).
[5]Z. K. Tang, G. K. L. Wong, P. Yu, M. Kawasaki, A. Ohtomo, H. Koinuma, and Y. Segawa, Appl. Phys. Lett. **72**, 3270 (1998).
[6]H. Ohta, M. Orita, M. Hirano, H. Tanji, H. Kawazoe, and H. Hosono, Appl. Phys. Lett. **76**, 2740 (2000).
[7]T. Makino, Y. Segawa, A. Tsukazaki, A. Ohtomo, and M. Kawasaki, Appl. Phys. Lett. **87**, 022101 (2005).
[8]K. Nomura, H. Ohta, K. Ueda, T. Kamiya, M. Hirano, and H. Hosono, Science **300**, 1269 (2003).
[9]T. I. Suzuki, A. Ohtomo, A. Tsukazaki, F. Sato, J. Nishii, H. Ohno, and M. Kawasaki, Adv. Mater. **16**, 1887 (2004).
[10]T. Miyasako, M. Senoo, and E. Tokumitsu, Appl. Phys. Lett. **86**, 162902 (2005).
[11]M. W. J. Prins, S. E. Zinnemers, J. F. M. Cillessen, and J. B. Giesbers, Appl. Phys. Lett. **70**, 458 (1997).
[12]J. Nishii, A. Ohtomo, K. Ohtani, H. Ohno, and M. Kawasaki, Jpn. J. Appl. Phys., Part 2 **44**, L1193 (2005).
[13]H. Y. Hwang, Y. Iwasa, M. Kawasaki, B. Keimer, N. Nagaosa, and Y. Tokura, Nat. Mater. **11**, 103 (2012).
[14]C. W. Bark, P. Sharma, Y. Wang, S. H. Baek, S. Lee, S. Ryu, C. M. Folkman, T. R. Paudel, A. Kumar, S. V. Kalinin, A. Sokolov, E. Y. Tsymbal, M. S. Rzchowski, A. Gruverman, and C. B. Eom, Nano Lett. **12**, 1765 (2012).
[15]H.-H. Wang, D.-F. Cui, S.-Y. Dai, H.-B. Lu, Y.-L. Zhou, Z.-H. Chen, and G.-Z. Yang, J. Appl. Phys. **90**, 4664 (2001).
[16]R. P. Wang and C. J. Tao, J. Cryst. Growth **245**, 63 (2002).
[17]H. J. Kim, U. Kim, H. M. Kim, T. H. Kim, H. S. Mun, B.-G. Jeon, K. T. Hong, W.-J. Lee, C. Ju, K. H. Kim, and K. Char, Appl. Phys. Express **5**, 061102 (2012).
[18]H. J. Kim, U. Kim, T. H. Kim, J. Kim, H. M. Kim, B.-G. Jeon, W.-J. Lee, H. S. Mun, K. T. Hong, J. Yu, K. Char, and K. H. Kim, Phys. Rev. B **86**, 165205 (2012).
[19]X. Luo, Y. S. Oh, A. Sirenko, P. Gao, T. A. Tyson, K. Char, and S.-W. Cheong, Appl. Phys. Lett. **100**, 172112 (2012).
[20]W.-J. Lee, H. J. Kim, E. Sohn, H. M. Kim, T. H. Kim, K. Char, J. H. Kim, and K. H. Kim, Phys. Status Solidi A **212**, 1487 (2015).
[21]H. Mun, U. Kim, H. M. Kim, C. Park, T. H. Kim, H. J. Kim, K. H. Kim, and K. Char, Appl. Phys. Lett. **102**, 252105 (2013).
[22]C. Park, U. Kim, C. J. Ju, J. S. Park, Y. M. Kim, and K. Char, Appl. Phys. Lett. **105**, 203503 (2014).
[23]H. J. Kim, J. Kim, T. H. Kim, W.-J. Lee, B.-G. Jeon, J.-Y. Park, W. S. Choi, D. W. Jeong, S. H. Lee, J. Yu, T. W. Noh, and K. H. Kim, Phys. Rev. B **88**, 125204 (2013).
[24]R. Schmid, Metall. Trans. B **14B**, 473 (1983).
[25]Z. Hiroi, M. Takano, M. Azuma, and Y. Takeda, Nature **364**, 315 (1993).
[26]B. A. Scott, J. R. Kirtley, D. Walker, B.-H. Chen, and Y. Wang, Nature **389**, 164 (1997).
[27]W.-J. Lee, E. Sohn, H. J. Kim, T. H. Kim, S. Sakong, D. Seo, J.-Y. Park, E. J. Choi, and K. H. Kim (unpublished).
[28]H. F. Wang, Q. Z. Liu, F. Chen, G. Y. Gao, W. Wu, and X. H. Chen, J. Appl. Phys. **101**, 106105 (2007).
[29]Q. Liu, J. Liu, B. Li, H. Li, G. Zhu, K. Dai, Z. Liu, P. Zhang, and J. Dai, Appl. Phys. Lett. **101**, 241901 (2012).
[30]E. H. Mountstevens, J. P. Attfield, and A. T. Redfern, J. Phys.: Condens. Matter **15**, 8315 (2003).
[31]H. Kim, J. S. Horwitz, S. B. Qadri, and D. B. Chrisey, Thin Solid Films **420–421**, 107 (2002).
[32]H. Toyosaki, M. Kawasaki, and Y. Tokura, Appl. Phys. Lett. **93**, 132109 (2008).
[33]T. Ohnishi, K. Shibuya, T. Yamamoto, and M. Kippmaa, J. Appl. Phys. **103**, 103703 (2008).
[34]T. Koida and M. Kondo, J. Appl. Phys. **101**, 063713 (2007).
[35]D. J. Keeble, B. Jalan, L. Ravelli, W. Egger, G. Kanda, and S. Stemmer, Appl. Phys. Lett. **99**, 232905 (2011).
[36]E. Ertekin, V. Srinivasan, J. Ravichandran, P. B. Rossen, W. Siemons, A. Majumdar, R. Ramesh, and J. C. Grossman, Phys. Rev. B **85**, 195460 (2012).